

## ***Supporting Information***

### Construction of core-shell MOF@COF hybrids with Z scheme heterojunction for efficient visible light photocatalysis

Jun Pang, Weijie Chen, Jintao Hu, Jie Cheng, Mingqiang Tang, Zewei Liu, and Rong Tan \*

National & Local Joint Engineering Laboratory for New Petro-chemical Materials and Fine Utilization of Resources; Key Laboratory of Chemical Biology and Traditional Chinese Medicine Research (Ministry of Education); Key Laboratory of the Assembly and Application of Organic Functional Molecules of Hunan Province, College of Chemistry & Chemical Engineering, Hunan Normal University, No.36, South Lushan Road, Changsha, Hunan 410081 (P. R. China).

#### **Corresponding Authors**

\* Rong Tan. E-mail: [yiyangtanrong@126.com](mailto:yiyangtanrong@126.com)

Number of pages: 11 (from S1 to S11)

Number of figures: 9

---

\* Corresponding authors. Fax: +86-731-88872531. Tel: +86-731-88872576

*E-mail:* [yiyangtanrong@126.com](mailto:yiyangtanrong@126.com)

**Content:**

1. Apparent quantum efficiency (AQE) for the formation of *N*-benzylidenebenzylamine over **NH<sub>2</sub>-UiO-66@TpBD-COF(21.9)**.
2. Determination of formed superoxide radical ( $\bullet\text{O}_2^-$ ), H<sub>2</sub>O<sub>2</sub>, and benzaldehyde during reaction.
3. Identification of the obtained imines.

1. Apparent quantum efficiency (AQE) for the formation of *N*-benzylidenebenzylamine over **NH<sub>2</sub>-UiO-66@TpBD-COF(21.9)**.

AQE at a variety of monochromatic visible light (400, 450, 550 or 650 nm) was obtained according to the yield of *N*-benzylidenebenzylamine over **NH<sub>2</sub>-UiO-66@TpBD-COF(21.9)** in 1 h.

The equation was as follow [1]:

$$\text{AQE} = \frac{n \times M \times N_A \times h \times c}{S \times P \times t \times \lambda} \times 100\%$$

Where *n* is the number of reaction electron (2 for benzylamine oxidation); *M* is the molar amounts of *N*-benzylidenebenzylamine formed; *N<sub>A</sub>* is the avogadro constant (6.022×10<sup>23</sup>); *h* is the Planck constant (6.626×10<sup>-34</sup> J·s); *c* is the speed of light (3.0×10<sup>8</sup> m/s); *S* is the irradiation area (6.25 cm<sup>2</sup>); *P* is the incident light intensity at certain wavelength (10.6, 27.3, 4432.6 and 239 mW/cm<sup>2</sup> for 400, 450, 550 and 650 nm, respectively); *t* is the irradiation time (3600 s); *λ* is the monochromatic light wavelength (400, 450, 550 and 650 nm). As expected, the change trend in AQE was consistent with that of light absorption strength of the **NH<sub>2</sub>-UiO-66@TpBD-COF(21.9)** (Table S1 and Fig. S1). The highest AQE reached to 10.0%, which was observed at 400 nm of monochromatic light irradiation.

Table S1. Calculated AQE of **NH<sub>2</sub>-UiO-66@TpBD-COF(21.9)** at different wavelength

<i>λ</i> (nm)	Yield of product (μmol)	<i>P</i> (mW/cm <sup>2</sup> )	AQE (%)
400	40	10.6	10.00
450	46	27.3	3.98
550	58	140.1	0.80
650	30	239.3	0.21

P: incident light intensity at certain wavelength

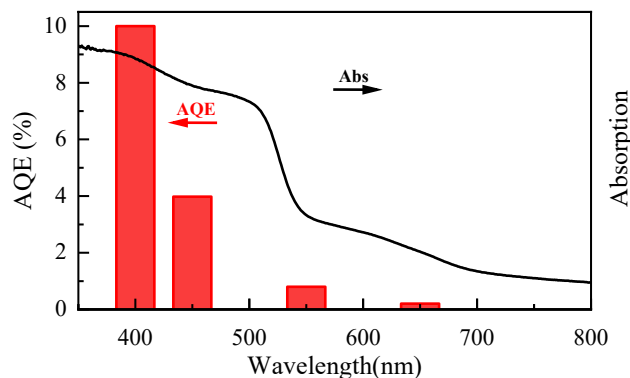


Fig. S1. The apparent quantum efficiency (AQE) for each wavelength of **NH<sub>2</sub>-UiO-66@TpBD-COF(21.9)**.

2. Determination of formed superoxide radical ( $\bullet\text{O}_2^-$ ),  $\text{H}_2\text{O}_2$ , and benzaldehyde during reaction.

2.1 Detection of superoxide radical ( $\bullet\text{O}_2^-$ ).

1,4-Bis(dimethylamino)benzene can be readily oxidized with molecular oxygen to form corresponding radical anion, accompanied by the reduction of oxygen to generate superoxide radical ( $\bullet\text{O}_2^-$ ). Thus, it was used as the detector of superoxide radical ( $\bullet\text{O}_2^-$ ).

The **NH<sub>2</sub>-UiO-66@TpBD-COF(21.9)** (10 mg) was ultrasonically dispersed in acetonitrile (2.5 mL) in a quartz glass vial. Benzylamine (0.2 mmol, 0.022 mL) and 1,4-bis(dimethylamino)benzene (0.048 mmol, 0.008 g) were added. The mixture was stirred for 30 min in dark to achieve the adsorption-desorption equilibrium of substrate. Afterward, a 35 W halogen lamp was illuminated from the reactor top to the reaction solution under magnetic stirring. The distance between lamp and reaction solution was approximately 7 cm. The reaction was performed at room temperature under ambient air. Aliquots at an interval of 1.0 h were drawn

from the reaction mixture to determine by UV-vis spectrophotometry. Obviously, as the reaction proceeds, an absorption peak (at 553 nm) ascribed to 1,4-bis(dimethylamino)benzene radical anion appears and gradually increases in UV-vis spectra of reaction mixture. It indicated the progressive oxidization of 1,4-bis(dimethylamino)benzene to corresponding radical anion, which was accompanied by the reduction of oxygen by photo-induced electron to generate superoxide radical ( $\cdot\text{O}_2^-$ ) (inset in Fig. S2-A) [2]. Notably, the peak didn't appear when catalyst is absence in the reaction. The results confirmed the ability of **NH<sub>2</sub>-UiO-66@TpBD-COF(x)** to mediate the electron transfer to oxygen to generate superoxide radical ( $\cdot\text{O}_2^-$ ).

## 2.2 Detection of H<sub>2</sub>O<sub>2</sub>.

*N,N*-Diethyl-1,4-phenylenediamine (DPD) was added to the reaction mixture to detect the generated H<sub>2</sub>O<sub>2</sub>, as DPD can be readily oxidized into DPD radical cation in the presence of H<sub>2</sub>O<sub>2</sub>.

The **NH<sub>2</sub>-UiO-66@TpBD-COF(21.9)** (10 mg) was ultrasonically dispersed in acetonitrile (2.5 mL) in a quartz glass vial. Benzylamine (0.2 mmol, 0.022 mL) and *N,N*-diethyl-1,4-phenylenediamine (DPD, 0.06 mmol, 0.01 mL) were added. The mixture was stirred for 30 min in dark to achieve the adsorption-desorption equilibrium of substrate. Afterward, a 35W halogen lamp was used as a light source and illuminated from the reactor top to the reaction solution under magnetic stirring. The distance between lamp and reaction solution was approximately 7 cm. The reaction was performed at room temperature the ambient air. Aliquots at an interval of 1.0 h were drawn from the reaction mixture to determine by UV-vis spectrophotometry. As shown in UV-vis absorption spectra in Fig. S2-B, with the addition of DPD in reaction mixture, new absorption peaks appears at 484 and 553 nm, which is ascribed to DPD radical cation. While, they didn't appear when **NH<sub>2</sub>-UiO-66@TpBD-COF(21.9)** is absence in the reaction. It suggests the

generation of  $\text{H}_2\text{O}_2$  in the photoredox aerobic oxidation [3].

### 2.3 Detection of benzaldehyde.

The  $\text{NH}_2\text{-UiO-66@TpBD-COF(21.9)}$  (10 mg) was ultrasonically dispersed in acetonitrile (2.5 mL). Benzylamine (0.2 mmol, 0.022 mL) was then added. The mixture was stirred for 30 min in dark to achieve the adsorption-desorption equilibrium of substrate. Afterward, a 35 W halogen lamp was used as a light source and illuminated from the reactor top to the reaction solution under magnetic stirring. The distance between lamp and reaction solution was approximately 7 cm. The reaction was performed at room temperature the ambient air. When the reaction was performed for 2 h, the reaction mixture was characterized by  $^1\text{H}$  NMR spectrum. As shown in  $^1\text{H}$  NMR spectrum in Fig. S2-C, an aldehyde group-associated proton signals is obvious at the positions of 10.05 ppm. It provided the convincing evidence for the formation of benzaldehyde as a reaction intermediate.

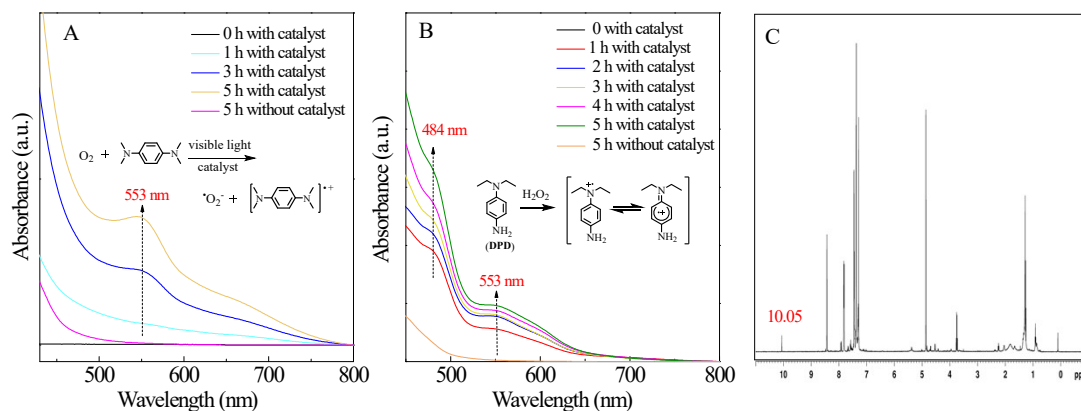


Fig. S2. (A) UV-vis spectra of 1,4-bis(dimethylamino)benzene radical anion generated by catalyst in the presence of visible light and oxygen, (B) UV-vis spectra of reaction mixture (benzylamine oxidation) with or without catalyst after adding DPD, (C)  $^1\text{H}$  NMR spectrum of the reaction mixture when the reaction was performed for 2 h. (catalyst:  $\text{NH}_2\text{-UiO-}$

**66@TpBD-COF(21.9)).**

### 3. Identification of the obtained imines

*N-Benzylidene-p-benzylamine (1)*: Crude product **1** was purified by chromatography on silica gel (petroleum ether/ ethyl acetate, 18: 1). Depurated product **1** was identified by  $^1\text{H}$  NMR spectrum (see Fig. S3).  $^1\text{H}$  NMR (500 MHz,  $\text{CDCl}_3$ )  $\delta$  (ppm): 8.43 (s, 1 H,  $\text{H-C=N}$ ), 7.82-7.80 (m, 2 H, Ph- $\text{H}$ ), 7.45-7.36 (m, 8 H, Ph- $\text{H}$ ), 4.86 (s, 2 H,  $-\text{CH}_2-$ ).

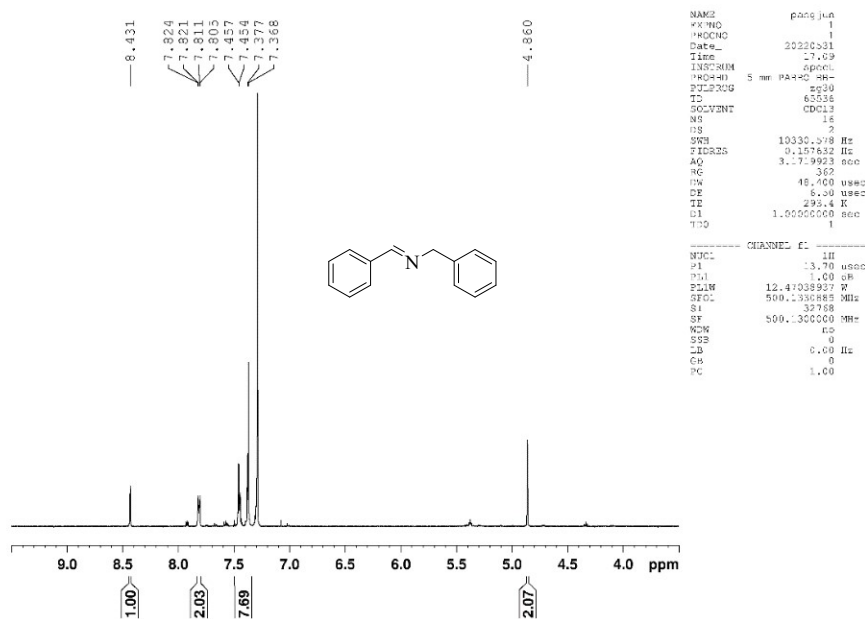


Fig. S3.  $^1\text{H}$  NMR spectrum of product **1**

*N-(4-Chlorobenzylidene)-p-Chlorobenzylamine (2)*: Crude product **2** was purified by chromatography on silica gel (petroleum ether/ethyl acetate, 15: 1). Depurated product **2** was identified by  $^1\text{H}$  NMR spectrum (see Fig. S4).  $^1\text{H}$  NMR (500 MHz,  $\text{CDCl}_3$ )  $\delta$  (ppm): 8.37 (s, 1 H,  $\text{H-C=N}$ ), 7.74-7.73 (d, 2 H, Ph- $\text{H}$ ), 7.43-7.41 (d, 2 H, Ph- $\text{H}$ ), 7.35-7.30 (m, 4 H, Ph- $\text{H}$ ), 4.79 (s, 2 H,  $-\text{CH}_2-$ ).

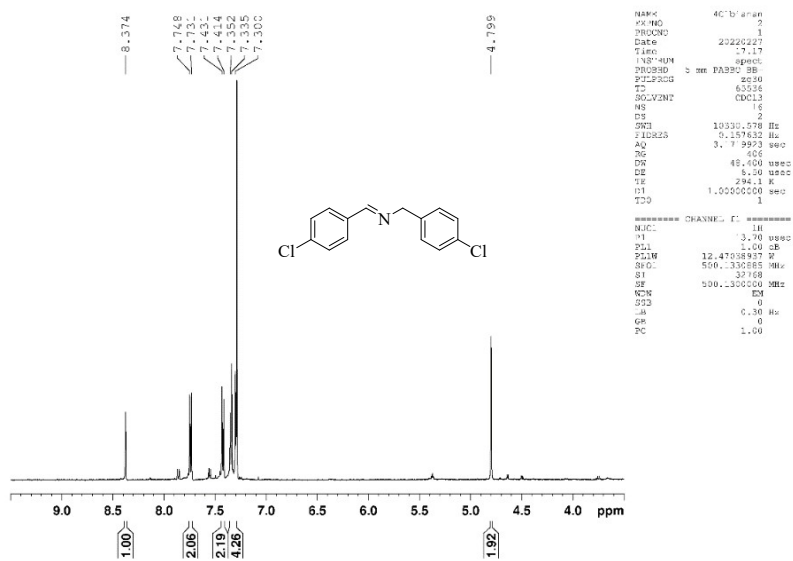


Fig. S4.  $^1\text{H}$  NMR spectrum of product **2**

*N*-(4-Fluorobenzylidene)-*p*-fluorobenzylamine (**3**): Crude product **3** was purified by chromatography on silica gel (petroleum ether/ethyl acetate, 15: 1). Depurated product **3** was identified by  $^1\text{H}$  NMR spectrum (see Fig. S5).  $^1\text{H}$  NMR (500 MHz,  $\text{CDCl}_3$ )  $\delta$  (ppm): 8.38 (s, 1 H,  $H\text{-C=N}$ ), 8.00-7.79 (d, 2 H, Ph- $H$ ), 7.33-7.32 (d, 2 H, Ph- $H$ ), 7.14-7.05 (m, 4 H, Ph- $H$ ), 4.79 (s, 2 H,  $\text{-CH}_2\text{-}$ ).

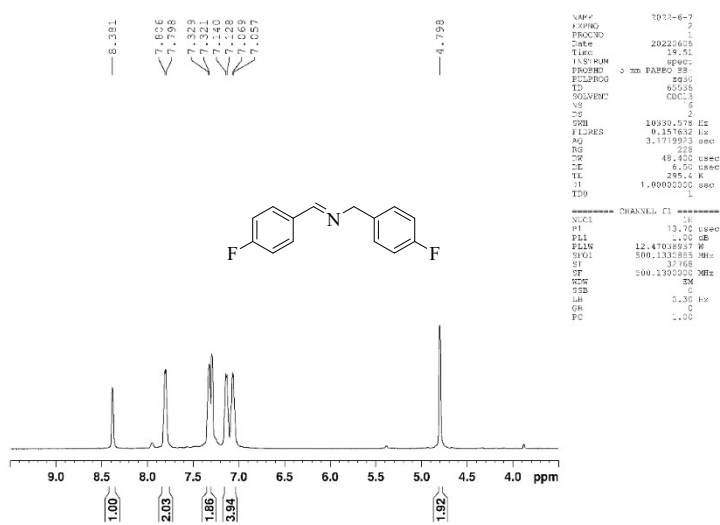


Fig. S5.  $^1\text{H}$  NMR spectrum of product **3**



*N*-(2-fluorobenzylidene)-*o*-fluorobenzylamine (**4**): Crude product **4** was purified by chromatography on silica gel (petroleum ether/ethyl acetate, 16: 1). Depurated product **4** was identified by <sup>1</sup>H NMR spectrum (see Fig. S6). <sup>1</sup>H NMR (500 MHz, CDCl<sub>3</sub>) δ (ppm): 8.76 (s, 1 H, *H*-C=N), 8.08-8.05 (m, 1 H, Ph-*H*), 7.46-7.45 (m, 2 H, Ph-*H*), 7.32-7.31 (t, 1 H, Ph-*H*), 7.22-7.07 (m, 4 H, Ph-*H*), 4.91 (s, 2 H, -CH<sub>2</sub>-).

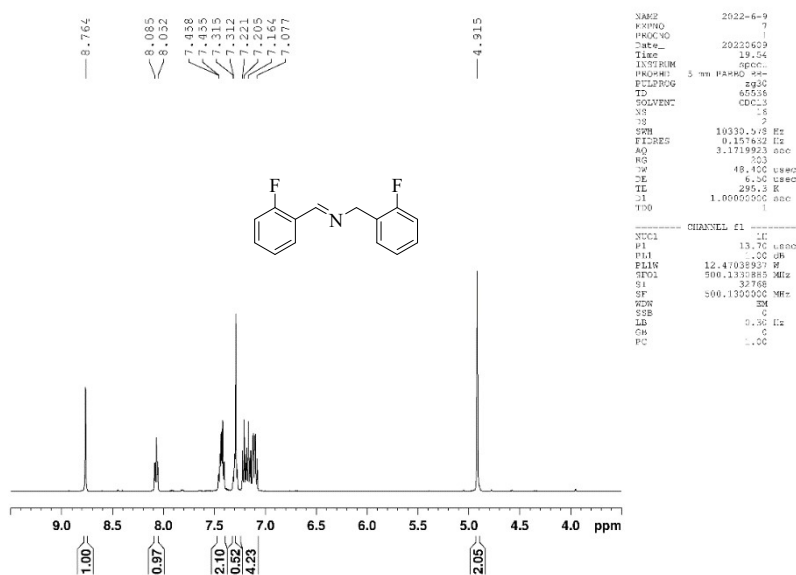


Fig. S6. <sup>1</sup>H NMR spectrum of product **4**

*N*-(4-(*tert*-Butyl)benzylidene)-*p*-(*tert*-butyl)benzylamine (**5**): Crude product **5** was purified by chromatography on silica gel (petroleum ether/ethyl acetate, 15: 1). Depurated product **2** was identified by <sup>1</sup>H NMR spectrum (see Fig. S7). <sup>1</sup>H NMR (500 MHz, CDCl<sub>3</sub>) δ (ppm): 8.39 (s, 1 H, *H*-C=N), 7.75-7.73 (d, 2 H, Ph-*H*), 7.4-7.45 (d, 2 H, Ph-*H*), 7.39-7.29 (m, 4 H, Ph-*H*), 4.81 (s, 2 H, -CH<sub>2</sub>-), 1.36-1.34 (d, 18 H, -C(CH<sub>3</sub>)<sub>3</sub>).

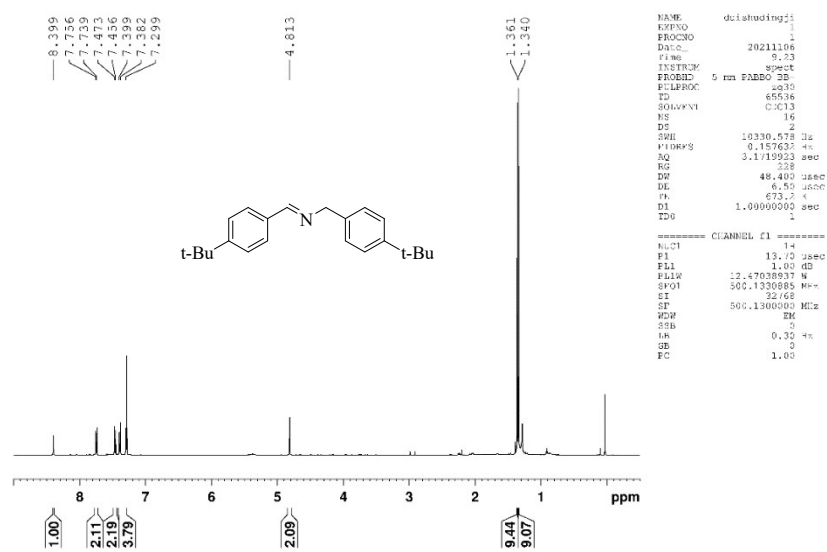


Fig. S7.  ${}^1\text{H}$  NMR spectrum of product **5**

*1-(Thiophen-2-yl)-N-(thiophen-2-ylmethyl)methanimine (6):* Crude product **6** was purified by chromatography on silica gel (petroleum ether/ethyl acetate, 16: 1). Depurated product **6** was identified by  ${}^1\text{H}$  NMR spectrum (see Fig. S8).  ${}^1\text{H}$  NMR (500 MHz,  $\text{CDCl}_3$ )  $\delta$  (ppm): 8.44 (s, 1 H,  $\text{H}-\text{C}=\text{N}$ ), 7.45-7.44 (d, 1 H,  $-\text{S}-\text{CH}=\text{C}=\text{N}$ ), 7.36-7.35 (d, 1 H,  $-\text{S}-\text{CH}=\text{C}=\text{N}$ ), 7.26 (s, 1 H,  $-\text{S}-\text{CH}=\text{C}=\text{N}$ ), 7.11-7.09 (t, 1 H,  $-\text{S}-\text{CH}=\text{C}=\text{N}$ ), 7.02-7.00 (m, 2 H,  $-\text{S}-\text{C}(\text{C}=\text{N})=\text{CH}-$ ), 4.97 (s, 2 H,  $-\text{CH}_2-$ ).

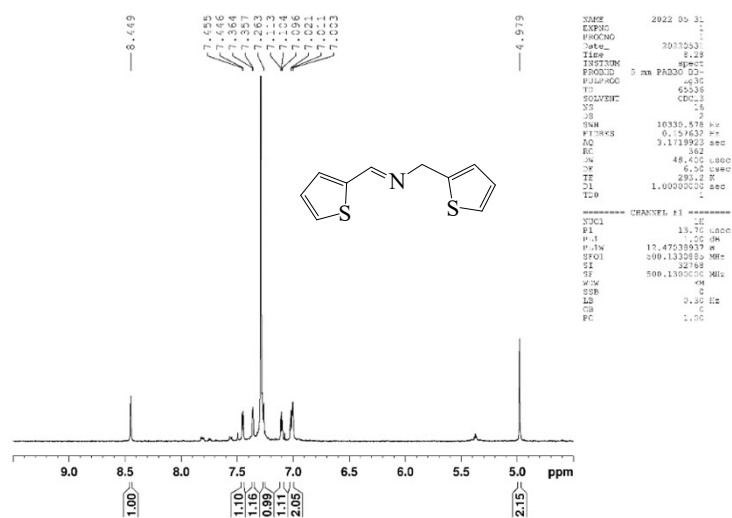


Fig. S8.  ${}^1\text{H}$  NMR spectrum of product **6**

*1-(Furan-2-yl)-N-(furan-2-ylmethyl)methanimine (7)*: Crude product **7** was purified by chromatography on silica gel (petroleum ether/ethyl acetate, 20: 1). Depurated product **7** was identified by <sup>1</sup>H NMR spectrum (see Fig. S9). <sup>1</sup>H NMR (500 MHz, CDCl<sub>3</sub>) δ (ppm): 8.14 (s, 1 H, *H*-C=N), 7.54 (s, 1 H, -O-CH=), 7.41-7.40 (d, 1 H, -O-CH=), 6.82-6.81 (d, 1H, -O-CH=CH-), 6.51-6.50 (t, 1 H, --O-CH=CH-), 6.37-6.36 (t, 2 H, -O-C(C=N)=CH-), 4.78 (s, 2 H, -CH<sub>2</sub>-).

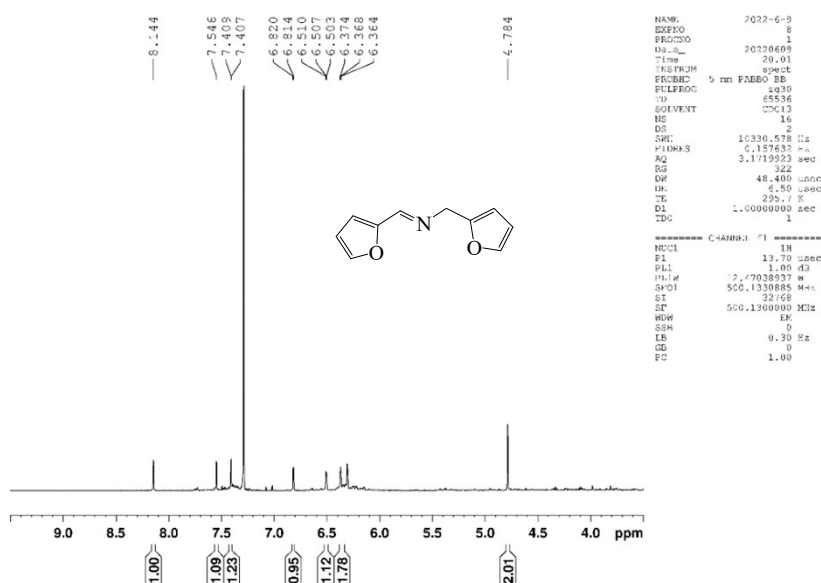


Fig. S9. <sup>1</sup>H NMR spectrum of product **7**

## References

- [1] J. Chen, H. Wang, Z. Zhang, L. Han, Y. Zhang, F. Gong, K. Xie, L. Xu, W. Song and S. Wu, J. Mater. Chem. A, 2019, 7, 5493-5503.
- [2] C. Su, R. Tandiana, B. Tian, A. Sengupta, W. Tang, J. Su and K.P. Loh, ACS Catal., 2016, 6, 3594-3599.
- [3] V.R. Battula, H. Singh, S. Kumar, I. Bala, S.K. Pal and K. Kailasam, ACS Catal., 2018, 8, 6751-6759.